ESTIMATION OF VEHICLE FLOOR PLATE LOADING AND RESPONSE DUE TO DETONATION OF A MINE SHALLOW-BURIED IN DRY SAND AND WET TUFF (U)

Aaron D. Gupta
U.S. Army Research Laboratory
Aberdeen Proving Ground, Maryland

ABSTRACT

(U) A mine-soil-structure interaction problem with a landmine buried in two different soil types was modeled using a hydrodynamic code. Because the actual soil types can vary widely between experiments, the problem was bracketed between two widely differing soil types—dry sand and fully saturated tuff. The ballistic pendulum anvil plate acts as a momentum trap for a vertical impulse measurement facility (VIMF) under development at Aberdeen Proving Ground, MD. The model allows simulation of complex asymmetric explosive-soil-structure interaction effects. It also generates loading and response of the plate due to varying offset, standoff, depth of soil overburden, and explosive contents.

(U) Introduction

(U) Both armored personnel carriers and light combat vehicles are increasingly being used in a support role for other, more heavily armored combat vehicles, all of which are being subjected to much greater risk from a variety of highly lethal antitank land mines. As a result, there is a need for modeling and understanding the interaction of mine blast products with structures and the resulting loading and damage mechanisms inflicted by explosive blast and impact. This understanding is required both for damage assessment and protective hardening of both wheeled and tracked vehicles. This has been a topic of considerable interest to the U.S. Army Research Laboratory (ARL) at Aberdeen Proving Ground, MD.

(U) An interesting study [1] involved collation of data from previous scaled experiments related to the encounter of buried land mines with various targets including flat plates. A correlation function, based on dimensional analysis, for the total impulse delivered by the land mine and overburden on a target was presented. Vulnerability of tank bottom hull floor plates subjected to shallow-buried mine blast was studied by Norman [2] and Hoskins et al. [3], who employed an approximate energy method approach and equated the strain energy absorbed by the plate to the energy delivered by the blast to the armor plate based on the law of conservation of energy. Various simple models of explosively driven metal were developed by Dehn [4] and compared with experiments.

(U) In another investigation [5], the DORF hydrocode was used to generate the loading history on a target plate subjected to a blast load from a land mine. The forcing function was used to compute the response of a clamped-edge square rolled homogeneous armor (RHA) plate using a structural response code. The predicted deflection and total impulse were in satisfactory agreement with values computed using an empirical correlation function derived from field experimental data.

(U) Dynamic response analysis of a rectangular simply supported plate subjected to an explosive blast was analyzed by Gupta [6] for the linear elastic case and compared to a closed-form solution. The analysis was extended to the elastic-plastic domain by Gupta et al. [7], who employed the isotropic bilinear hardening material model available in the ADINA nonlinear finite element analysis code. This study was further extended by Gupta et al. [8] to the response of a generic vehicle floor model subjected to empirically obtained triangular overpressure loads from the detonation of a shallow-buried mine. Although qualitative agreement with experiment for peak deflection could be obtained, the residual plastic deformation could not be compared effectively due to lack of soil loading arising from blast-soil-structure interaction, which substantially affected the estimated blast loads and the resultant structural response. Another recent study of dynamic elastic-plastic stress and deformation response of a generic vehicle floor model to coupled blast and impact loads from a plate mine was reported by Gupta [9], who provided an inexpensive method of evaluation of the structural integrity of modern vehicles subjected to severe spatially varying transient loads in extreme environments.

(U) A number of studies have been performed in the general area of blast response to structures over the years. However, the loading mechanisms from explosive blast-soil-structure interaction such as those occurring from detonation of a buried mine below a vehicle are poorly understood at present. The current investigation is an attempt to fill this void and to simulate loading of the anvil plate, which acts as a momentum trap due to an off-centered mine explosion and subsequent blast-soil-structure interaction resulting in target rotation and vertical displacements needed for the design of the guide shaft for the Vertical Impulse Measurement Facility (VIMF).

(U) Objective

(U) The primary objective of this investigation is to simulate detonation of a mine buried

in two different soil types—saturated tuff and dry sand. The shallow-buried mine detonation causes motion of the soil media and propagation of the blast-soil wave upward, resulting in blast-soil-structure interaction and consequent loading of the anvil plate, which is employed as a momentum trap. The study is necessitated by the need to obtain improved loading functions for combined blast and soil loading under extreme loading conditions and bracket the influence of soil properties upon the loading and response of the ballistic pendulum anvil plate between two differing soil types and moisture contents. These loading data can then be transferred to a nonlinear finite element analysis code to yield transient structural response including deformation, displacement, and rotation of a representative structural element. The predicted results could then be compared to data from experiments designed to capture and measure the loads produced in these events in a severe environment. Such capability will, in turn, enable the development of models of expansion of blast/soil events in which soil properties play a significant role.

(U) Accuracy of predictive models is essential to the development of innovative vehicle designs that have improved survivability characteristics and are, at the same time, light enough to ensure rapid deployment and desired load-carrying capacity. The ultimate objective is to improve survivability of crew in vehicles subject to land mine attack.

(U) Problem Configuration

(U) The problem involves the worst-case scenario of a shallow-buried cylindrical mine embedded all around in two different soil types: dry sand and wet soil with a 15-cm soil overburden. The mine contains explosive with an equivalent charge weight of 10 kg TNT and is asymmetrically located with a horizontal centerline offset distance of 61 cm relative to a square plate 244 cm H 244 cm. Plate thicknesses of 15 cm and 20 cm were modeled. The vertical standoff between the bottom plate surface and the top of the soil overburden was 41 cm as shown in Figure 1. The cylindrical configuration of the mine has a diameter of 32 cm and a height of 9 cm. The mine is located inside a block of soil 366 cm in diameter with a total height of 124 cm.

(U) Basic Assumptions

(U) The asymmetric configuration of the mine as defined in the previous section is a three-dimensional (3-D) problem requiring the generation of a 3-D model that is expensive to run using a hydrodynamic code. The model was simplified using two-dimensional (2-D) plane strain assumptions. In this model, lateral dimensions of the plate, the mine, and the soil enclosure perpendicular to the X-Y plane were assumed to extend to infinity.

(U) The mine is assumed to consist of a bare charge without the presence of a metallic casing. The relatively small mass of the casing would not significantly contribute to the resultant impulse or momentum absorbed by the momentum trap. The plate is expected to undergo minimal deformation in order that displacements and rotations can be easily tracked and compared with experiments.

UNCLASSIFIED

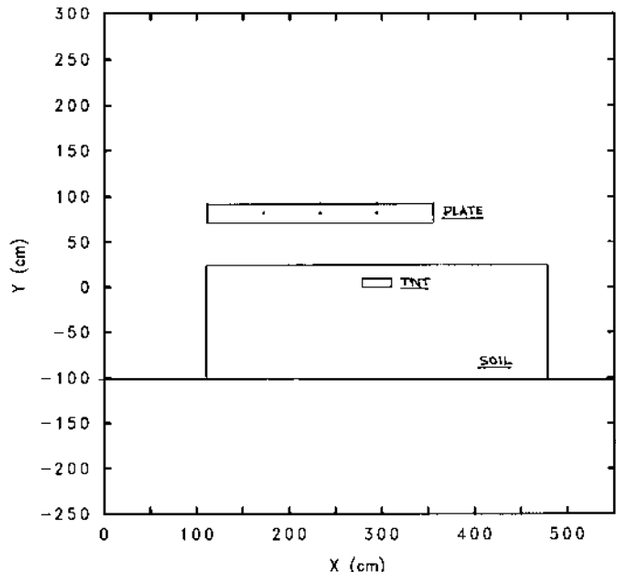

Figure 1. (U) Initial Configuration of the Mine-Soil-Structure Interaction Problem

UNCLASSIFIED

(U) All empty spaces between the plate and the soil block and all around these configurations were filled with dry air in the hydrocode model. The fully saturated tuff is assumed to be strongly clumped together due to high moisture content completely filling the void volume, which is approximately 30% of the entire soil volume. This ensures a worst-case scenario with significant contribution to the resultant momentum produced in the momentum trap. In the second case, dry sand with no moisture content is considered as the burial medium. This allows bracketing of the influence of large variation of soil properties and moisture contents upon structural loading and response between two widely varying soil types.

(U) Model Description

(U) A 2-D asymmetric model with a 61-cm centerline offset of the anvil plate, as shown in Figure 1, was generated for the CTH code. A 2-D Eulerian mesh was overlaid using uniform grid spacing in both horizontal and vertical directions throughout the computational space. Each cell size was a square mesh 1 cm × 1 cm, and the total number of cells was 165,000. An aspect ratio of 1.0 was maintained in computational space to ensure numerical accuracy. The problem region was extended approximately 110 cm vertically above the top plate surface and horizontally beyond the left and right geometric edges to minimize reflection from the computational boundaries. This large

volume of space filled with dry air accommodated large displacements and tilt angles of the anvil plate expected to occur due to asymmetric loading from mine detonation. Computed prediction of peak vertical displacements and rotation will be useful in designing vertical guides, guide bars, and springs for the experimental test fixture.

(U) Boundary Conditions

(U) The steel plate is assumed to be freely suspended 46 cm above the top surface of the soil block in which the mine is embedded and is initially at rest. The bottom horizontal soil boundary 100 cm below the mine is assigned a transmitting boundary condition where mass may flow in and out of mesh but no reflection is allowed from the boundary.

(U) Both left and right vertical as well as the top horizontal boundaries of the computational mesh are assigned extrapolated pressure boundary conditions where mass is not allowed to flow into the mesh but the pressures in cells at the boundary are computed using extrapolated values from two adjacent cells. This boundary condition is mostly transmissive with some reflection permitted.

(U) Material Models

(U) The model involves four different material types. The first package in the problem setup represents the TNT explosive for the land mine. The next package represents the rolled homogeneous armor (RHA) steel plate. This is followed by the soil package surrounding the explosive. The final package refers to dry air, which is used to fill all remaining empty space between and around the previous three packages and extends up to the edges of the computational mesh.

(U) The Mie-Grüneisen equation of state for steel available from the CTH code [10] material library was used to model the anvil plate. The corresponding response of the plate appeared to be highly dependent on material density rather than the assigned Grüneisen coefficients, and no attempt was made to improve upon these coefficients to better represent the RHA steel.

(U) Initially, the Johnson-Cook [11] constitutive model for the deviatoric response behavior of steel was used, which resulted in appreciable transverse bending deformation of the steel plate. To simulate nearly rigid deformation response of the steel plate, an elastic-perfectly plastic constitutive relationship with a high yield point and a high initial elastic modulus was used. This model appeared to work reasonably well since rigid-body translation and rotation of the steel plate were of primary interest.

(U) The material model employed for the TNT explosive was the JWL (Jones-Wilkins-Lee) equation of state available in the material library. For the detonation of the explosive, an explosive burn routine designated as HEBURN in the hydrocode was employed. The initiation was chosen to start at the bottom central location on the vertical symmetry axis of the mine, and pressure contour plots were generated at a regular interval of 10-cm radius.

(U) The soil material models were rather difficult to select because of limited information available on dynamic soil properties of widely differing soil types at high strain rates. Soil properties appear to vary considerably depending upon the location, type, moisture content, porosity, aggregate size, ambient temperature, and humidity conditions, etc. These property variations can significantly affect the interacting loading mechanisms and generated load functions as well as the resultant structural response. Most dynamic soil equations of state are devoted to high compression regimes appropriate in underground tests, and very little information is available for soil models in tension or dilatation as occurs in shallow-buried mine explosions.

(U) After consideration of various soil types, two different soil types were selected to bracket the problem between two limiting soil conditions. The soil types selected were fully saturated tuff designated as WTUFF and dry sand whose material models are available in the CTH Seslan material library. The equation of state for wet tuff has all voids filled with water. The void volume is approximately 30% of the total volume. The soil is assumed to remain clumped together during blast propagation and interaction with the target for a considerable period of time until the combined soil and blast products flow past the target corners and envelop the front and side surfaces of the anvil plate. Reasonably high fracture strength was specified for WTUFF to minimize severe fragmentation of the soil and allow maximum vertical momentum to be imparted to the anvil plate. The yield strength for wet soil was set at a realistic value, which was an order in magnitude lower than the fracture strength.

(U) The equation of state for dry sand available in the material library was similar to quartz crystal with an initial density of 2.6 cm^3, which was deemed to be too high. The dry sand appeared to behave like a rock with high density and stiffness properties. The high density and low porosity contributed to unrealistic mass and momentum to be imparted to the anvil plate acting as a momentum trap. The porosity ratio was reset at 1.45 in the model, and the CTHGEN preprocessor was rerun to produce the correct density and mass, plus a pressure that was essentially ambient. After model verification, CTH was rerun with the improved dry sand model. Since the dry sand was initially in contact with the mine at rest, it evolved along with the blast wave from mine detonation. The resultant blast-soil wave propagated together toward the anvil plate, and numerical instability was not a problem.

(U) Response Computation

(U) The simulation of the propagation of the explosive blast and soil products through the air and of the subsequent interaction with the steel plate was performed using the CTH hydrodynamic code. An initial time step of 1.0 μs was selected at the start of computation, and the response was tracked up to 2 ms, corresponding to approximately 2,000 computational cycles. A minimum time step of 0.01 μs was specified to avoid numerical instability.

(U) Gravity effects were included in the simulation to duplicate actual experimental conditions. Active Lagrangian tracer particles were selected along the back surface and the

horizontal midplane as well as the vertical axis of symmetry of the plate. The selection of tracer particles where history plots of position, velocity, pressure, and maximum principal stress as a function of time would be generated was guided by experimental considerations. The locations selected generally corresponded with locations where gauges were to be mounted.

(U) History plots of vertical linear momentum trapped in the RHA steel plate were generated for later comparison with momentum measurements. Cross-sectional plots of blast-soil-structure interaction and target response were plotted at frequent time intervals. These graphical representations led to a better understanding of the loading mechanisms.

(U) Results and Discussions

(U) Cross-sectional plots of blast-soil-plate interaction revealed elongation of steel plate at bottom corners in spite of high elastic modulus and stiffness properties of the RHA steel. Corner deformation was found to be an artifact of the numerical code computation, occurring at or near the interface where a mesh containing a relatively stiff material is located next to a soft material. This condition caused uncontrolled material flow and leakage through corners along the interface. It was decided to use the boundary layer interface (BLINT) capability in the code along the interface between the hard RHA steel target and the relatively soft air medium to mitigate this problem. However, no significant change was observed in the resultant time history or cross-sectional plots due to use of the BLINT capability available in the hydrocode.

(U) Two alternative plate thicknesses—15 cm and 20 cm—were considered. The objective was to find an optimum thickness for the anvil plate capable of trapping the momentum without significant bending deformation but yet yielding measurable rise in height. Computation using the 15-cm-thick anvil plate exhibited significant bending deformation, a typical cross-sectional view of which is shown in Figure 2. The amount of deformation observed was deemed unacceptable.

(U) Computations using the 20-cm-thick plate exhibit only minimal bending deformation, a typical cross-sectional plot of which is shown in Figure 3. This figure also depicts visible tilting of the plate. Both vertical and horizontal displacements of tracers on the rear surface, midplane, and the vertical plate symmetry axis were generated to facilitate calculation of peak displacements and tilt angles of the plate at specific response times.

(U) A typical history plot of integrated linear momenta in the vertical Y direction for the steel plate is shown in Figure 4. The momentum is initially 0 for the first 0.5 ms until the arrival of the blast wave at the bottom interface of the plate. The momentum absorbed by the plate increases rapidly for the next 0.1 ms and then gradually for an additional 1.4 ms. Thereafter, it reaches a plateau before eventually decaying due to air drag and gravitational effects. Comparison of the anvil plate vertical momenta from detonation of a mine buried in saturated tuff (shown as a curve joining filled diamonds) vs. dry sand (described by a curve joining square boxes) indicates consistently higher momenta for wet tuff relative to dry sand attaining a peak differential of between approximately 25% and 30% as shown in Figure 4. This is not unexpected since dry sand has a significantly lower density

than wet tuff, which remains cohesive for a considerable period of time before fragmentation while
UNCLASSIFIED

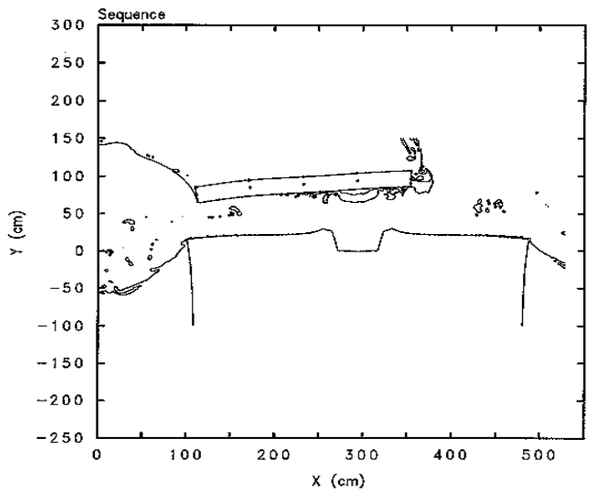

Figure 2. (U) A Sectional View of the Mine-Soil-Plate Interaction at 2 ms for the 15-cm-Thick Plate

UNCLASSIFIED

UNCLASSIFIED

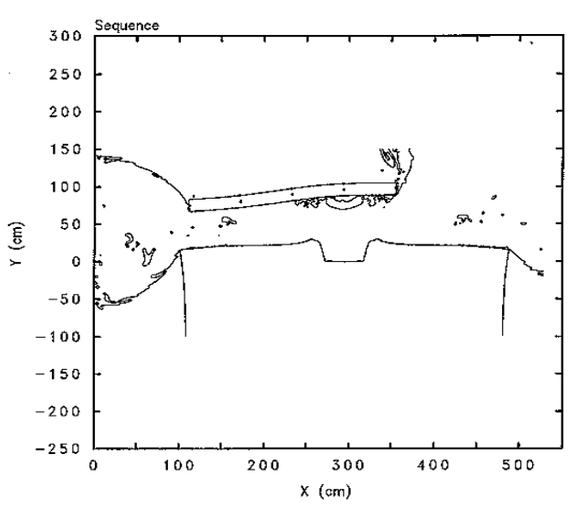

Figure 3. (U) A Sectional View of the Mine-Soil-Plate Interaction at 2 ms for the 20-cm-Thick Plate

UNCLASSIFIED

UNCLASSIFIED

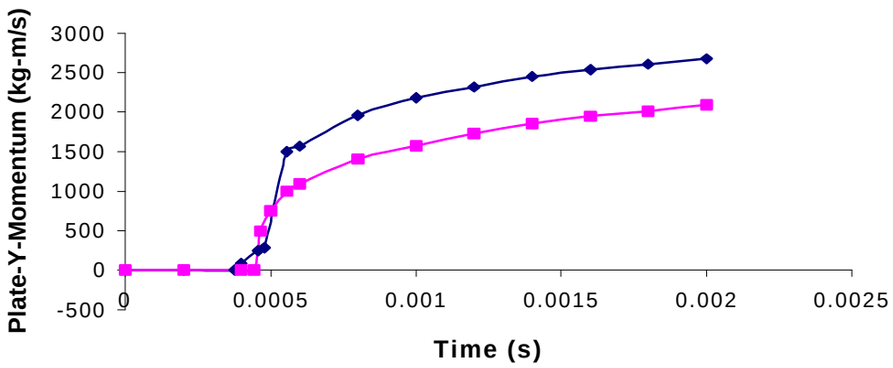

Figure 4. (U) Comparison of Plate Vertical Momentum From Detonation of Mine Buried in Wet Tuff vs. Dry Sand

UNCLASSIFIED

lighter sand particles have low mass and momentum and tend to separate earlier before reaching the plate surface.

(U) Section plots of explosive detonation and progression of blast waves leading to interaction with soil ejecta and the anvil plate as well as history plots of pressure, velocity, stress, and impulse are available but are not presented here due to space limitation. However, these plots indicate a thin layer of soil located near the leading edge of the blast wave, which is eventually compressed and flattened out against the anvil plate. Subsequently, the blast wave front branches out laterally along the plate interface until it reaches the bottom plate corners on either side. The wave then flows around these corners and envelops the plate. The bottom right corner is engulfed first because of its proximity to the wave front due to asymmetric location of the plate relative to the buried explosive. The asymmetric nature of blast wave interaction with the plate results in nonuniform loading of the plate. This leads to angular tilting, which is clearly visible in Figure 5.

(U) The vertical rise of the anvil plate due to entrapment of the linear vertical momentum shown in Figure 4 is accompanied by simultaneous rotation of the plate due to asymmetric loading of the plate from the blast-soil-structure interaction. The amount of rotation of the plate could not be predicted explicitly by the CTH code. However, data output tables of both vertical and horizontal locations of the tracer particles numbered 1–5 on the central horizontal plate axis, with respect to time, could be generated easily in a two-column ASCII format in CTH and readily transferred to Excel 97. A straight line equation of the form y = mx + c (where m is the gradient and c is the intercept) was fitted at each selected response time. Angular rotation of the fitted line was calculated in radians and converted to degrees from the relationship of the form m = tan[(180/pi) H theta],

UNCLASSIFIED

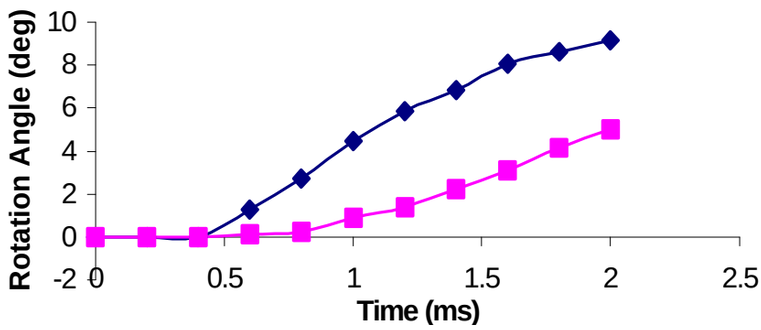

Figure 5. (U) Comparison of Rotation Angles Between 15-cm and 20-cm-Thick RHA Plates vs. Time Due to Detonation of a Mine Buried in Saturated Tuff

UNCLASSIFIED

where theta is the angle of rotation. Plots of rotational angles of the plate median axis with time for the 20-cm-thick plate vs. the 15-cm-thick plate due to detonation of the mine buried in wet tuff were generated in Excel and superimposed as shown in Figure 5. The curve connecting rectangular-filled boxes refer to the 20-cm-thick plate while the other curve represents the 15-cm-thick plate. Peak tilt angle for the 15-cm-thick plate was nearly twice the peak angle for the 20-cm-thick plate. Comparison of angular tilt for the 20-cm-thick plate due to the mine embedded in dry sand vs. wet tuff is shown in Figure 6. Although the plate shows higher tilting initially due to mine detonation in sand due to early arrival of lighter sand particles, at later times plate rotation due to mine detonation in wet tuff is clearly higher when compared to the response due to sand due to increased mass and momentum of saturated tuff both along vertical and horizontal directions.

(U) The peak vertical rise of the momentum trap at the midpoint on the axis of symmetry of the plate was obtained from the CTH data output table at the Lagrangian tracer particles by subtracting the initial y-position data from the final vertical location of the tracer particle 3 at 2 ms for both 20-cm-thick and 15-cm-thick plates. The results were tabulated and plotted in Excel 4, and the resultant plot is shown in Figure 6. A linear interpolation has been assumed between these data points, but this may change as more data become available. The vertical momentum plot in Figure 4 reaches a plateau at 2 ms, at which point acceleration is vanishingly small but the residual velocity due to inertia of the plate will continue to allow the plate to rise further until gravity brings the plate to a halt and reverses direction of motion as the plate starts to fall until it returns to the initial position. The 244-cm H 244-cm H 15-cm plate has a total mass of 6,770 kg and a vertical rise of 10.78 cm while the 244-cm H 244-cm H 20-cm plate has a total mass of 9,030 kg and a vertical rise of 7.66 cm at 2 ms. As expected, the thicker plate with an increased mass and moment of inertia

attains a smaller vertical rise at 2 ms as shown in Figure 7.

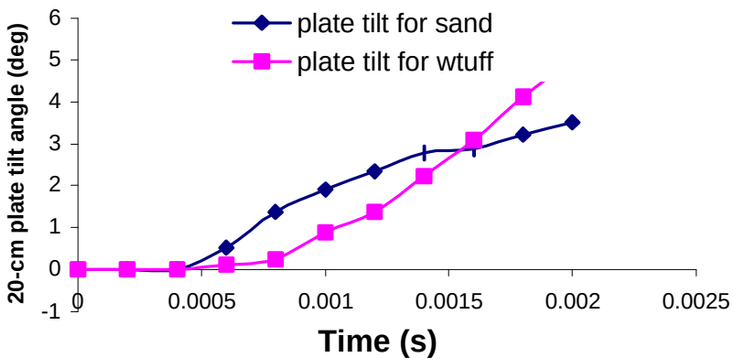

Figure 6. (U) Comparison of 20-cm Plate Rotation Due to Mine Detonation in Dry Sand vs. Wet Tuff

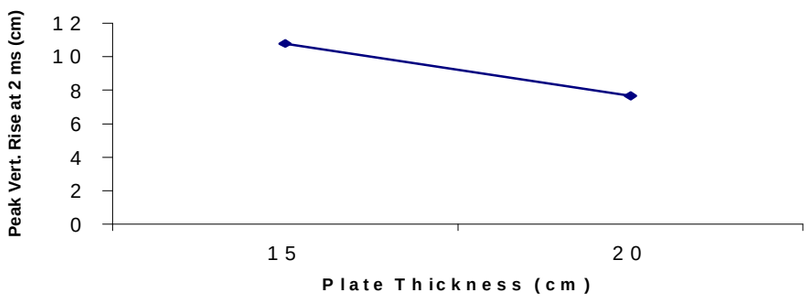

Figure 7. (U) Peak Vertical Rise of the Momentum Trap vs. Plate Thickness at 2 ms

(U) Conclusions and Recommendation

(U) The 20-cm-thick RHA plate experienced minimal transient deformation but incurred a severe weight penalty. To minimize weight, two plates with a total thickness of 10 cm were used. The loss of stiffness was compensated using two 5-cm-thick plates connected to I-beams in between with approximately equivalent stiffness of a 20-cm-monolithic plate. This design has the benefit of

easy replacement of the bottom parasitic plate, which is subjected to permanent damage from repeated tests without having to replace the entire momentum trap.

(U) The selection of soil properties in this study was limited to only two types of soil—dry sand and wet tuff—which were representative of two widely differing soil types and moisture conditions and limited the problem between fully dry and fully saturated soil media. The selection of soil properties must be broadened to include other types of soil with differing moisture contents and porosity. The soil fracture properties need to be improved particularly to include granularity and realistic soil fragmentation as well as ejecta formation. Further parametric studies should be conducted to include different types of landmines with varying types and contents of explosive. Additionally, the effect of varying standoff and offset distances on plate response behavior should be studied and compared with experiments for purposes of model validation. Once these effects are well understood and confidence is gained in modeling and simulation of mine-soil-structure interaction problems, improved design for blast mitigation and crew protection from land mines is feasible.

(U) Acknowledgements

(U) This project was undertaken as a part of a program involving land mine effects on structures. The valuable assistance of N. Gniazdowski, P. Kingman, and F. Gregory, of Weapons and Materials Research Directorate, and S. Betten, a George Washington University Science and Engineering Apprentice at ARL, during the course of this investigation is gratefully acknowledged.

(U) References

1. (U) Hanna, J. W. "An Effectiveness Evaluation of Several Types of Antitank Mines." BRL-MR-616, U.S. Army Research Laboratory, Aberdeen Proving Ground, MD, 1952 (UNCLASSIFIED).

2. (U) Norman, R. M. "Deformation in Flat Plates Exposed to HE Mine Blast." AMSAA-TM-74, U.S. Army Materiel Systems Analysis Agency, Aberdeen Proving Ground, MD, 1970 (UNCLASSIFIED).

3. (U) Hoskin, N. E., J. W. Allan, W. A. Bailey, J. W. Lethaby, and I. Skidmore. "The Motion of Plates and Cylinders Driven at Tangential Incidence." *Fourth International Symposium on Detonation,* ACR-126, Office of Naval Research, Pasadena, CA, 1965 (UNCLASSIFIED).

4. (U) Dehn, J. T. "Models of Explosively Driven Metal." BRL-TR-2626, U.S. Army Research Laboratory, Aberdeen Proving Ground, MD, 1984 (UNCLASSIFIED).

5. (U) Lottero, R. E., and K. D. Kimsey. "A Comparison of Computed Versus Experimental; Loading and Response of a Flat Plate Subjected to a Mine Blast." BRL-MR-02807, U.S. Army Research Laboratory, Aberdeen Proving Ground, MD, 1984 (UNCLASSIFIED).

6. (U) Gupta, A. D. "Dynamic Analysis of a Plate Subjected to an Explosive Blast." *Proceedings of the ASME International Computers in Engineering Conference and Exhibition*, vol. 1, Boston, MA, 1985 (UNCLASSIFIED).

7. (U) Gupta, A. D., F. H. Gregory, R. L. Bitting, and S. Bhattacharya. "Dynamic Analysis of an Explosively Loaded Hinged Rectangular Plate." *Computers and Structures*, vol. 26, pp. 339–344, United Kingdom: Pergamon Press Ltd., 1987 (UNCLASSIFIED).

8. (U) Gupta, A. D., H. L. Wisniewski, and R. L. Bitting. "Response of a Generic Vehicle Floor Model to Triangular Overpressure Loads." *Computers and Structures*, vol. 32, no. 3/4, pp. 527–536, United Kingdom: Pergamon Press Ltd., 1989 (UNCLASSIFIED).

9. (U) Gupta, A. D. "Dynamic Elasto-plastic Response of a Generic Vehicle Floor Model to Coupled Transient Loads." PVP-Vol. 351. *Structures Under Extreme Loading Conditions*, pp. 81-86, ASME, 1997 (UNCLASSIFIED).

10. (U) McGlaun, J. M., S. L. Thompson, and M. G. Elrick. "CTH: A Three-Dimensional Shock Wave Physics Code." *International Journal of Impact Engineering*, vol. 10, nos. 1–4, pp. 251–360, 1990 (UNCLASSIFIED).

11. (U) Johnson, G. R., and W. H. Cook. "A Constitutive Model and Data Subjected to Large Strains, High Strain Rates and High Temperatures." *Proceedings of the Seventh International Symposium on Ballistics*, pp. 541–547, The Hague, Netherlands, 1983 (UNCLASSIFIED).